

Production and Annihilation of an Antiproton in a Nuclear Emulsion*

R. D. HILL, STIG D. JOHANSSON, AND F. T. GARDNER
Physics Department, University of Illinois, Urbana, Illinois
 (Received March 26, 1956)

A track connecting two high-energy stars in a nuclear emulsion has been identified as an antiproton. Ionization density and scattering measurements on the track indicate that the antiproton's energy was 710 ± 150 Mev, whereas the energy in the secondary star caused by the antiproton was certainly greater than 1460 Mev. The stars in which the antiproton originated and was annihilated are described.

A PRELIMINARY report of an event which showed the probable production and annihilation of an antiproton has been given.¹ At the time of this report, the star in which the antiproton was produced had not been analyzed and the antiproton track had not then been critically examined for evidence of multiple scattering. The complete analysis now supports more strongly the identification as an antiproton, and we believe it may be of interest to report the details of the production and annihilation of an antiproton in this particular event.

PRODUCTION STAR

The production star, *A*, is a $9+4p$ star produced by a 6.2-Bev proton accelerated in the Berkeley Bevatron. A diagram of the star, showing prong numbers, is given in Fig. 1, and details of the measurement on the prongs are given in Table I.

Wherever the tracks did not end in the emulsion, ionization measurements were combined with scattering and/or range observations in order to identify the tracks. Confirmation of the ionization—scattering identification was obtained from variation of ionization density vs range for tracks 3 and 10 of star *A* and for five cases of star *B*. We feel reasonably confident therefore that the identification from ionization—scattering alone of

the three π mesons in star *A* is reliable. These tracks, 8, 13, and 14, do not dip excessively steeply for scattering measurements and there is good agreement of the $p\beta$ values obtained from ionization and scattering measurements. Had these tracks been protons, their $p\beta$ values obtained from ionization observations would have been between 1 and 4 Bev/c, which are very much higher than the scattering values observed.

Track 4, which breaks up into a hammer track at its end, appears to be a Li^8 fragment. A slow electron emerges from the center of the hammer, and from the equal lengths of the hammer prongs we estimate a Q of 9.1 Mev, which is consistent with the known decay of Be^8 . From the fact that eight protons are observed in star *A* and the recognition of Li^8 as one of the products of the star, we may conclude that the disintegrating nucleus was probably heavier than O^{16} .

The energies of the tracks from star *A* have been estimated, when the tracks stopped in the emulsion, from range-energy values,² and when the tracks left the emulsion, from ionization density—energy data.³ The total energies of the particles are given in the final column of Table I. A value of 8-Mev binding energy has been added to the kinetic energy of a proton, and a rest energy of 140 Mev has been added to the kinetic energy

TABLE I. Details of tracks in star *A*.

Track	Identity	Range	Plates	Dip angle ^a	Space angle to track No. 1.	Grain or blob count ^b	Ionization $p\beta$ (Mev/c)	Scattering $p\beta$ (Mev/c)	Momentum (Mev/c)	Energy (Mev)	Total energy (Mev)
1	p	3°	...	0.95 b_p	7076	6200	
2	p	548 μ	20-21	35°	49°	138	10.1	18.1
3	p	>11.3 mm	20-1	43°	61°	(2.27 \pm 0.12) g_p	(280 \pm 40)	(280 $_{-100}^{+200}$)	557	153	161
4	Li^8	19 μ	20	36°	68°	360	8.8	8.8
5	p	643 μ	20	1°	63°	144	11.0	19.0
6	p	161 μ	20	69°	78°	95	4.8	12.8
7	p	>7.6 mm	20-24	13°	165°	(1.72 \pm 0.07) g_p	(510 \pm 50)	(505 $_{-85}^{+130}$)	793	290	298
8	π	>4.9 mm	20-24	20°	165°	(0.93 \pm 0.04) b_p	(370 $_{-100}^{+200}$)	(280 $_{-60}^{+90}$)	402	286	426
9	\bar{p}	(1.4 mm)	20	0.02°	172°	(1.09 \pm 0.05) b_p	(1115 \pm 150)	(750 $_{-240}^{+670}$)	1355	710	2586
10	p	>2.9 mm	20-24	32°	152°	(2.56 \pm 0.1) g_p	(240 \pm 20)	(145 $_{-40}^{+80}$)	496	123	131
11	p	74 μ	20,21	58°	127°	75	3.0	11.0
12	p	6 μ	20	0°	149°	32	0.5	8.5
13	π	>14.7 mm	20-1	33°	123°	(0.95 \pm 0.03) b_p	(280 $_{-20}^{+100}$)	(210 $_{-70}^{+180}$)	323	212	352
14	π	>22.5 mm	20-4	22°	114°	(1.15 \pm 0.04) b_p	(130 \pm 10)	(155 $_{-20}^{+60}$)	177	86	226

^a Dip angles are in the undeveloped emulsion.
^b b_p and g_p refer to the plateau values of blob and grain densities, respectively.

* Assisted by the joint program of the Office of Naval Research and the U. S. Atomic Energy Commission.

¹ Hill, Johansson, and Gardner, Phys. Rev. **101**, 907 (1956).

² Baroni, Castagnoli, Cortini, Franzinetti, and Manfredini, C.E.R.N. Document BS9 (unpublished).

³ B. Judek and E. Pickup, private communication; A. Husain and E. Pickup, Phys. Rev. **98**, 136 (1955); J. R. Fleming and J. J. Lord, Phys. Rev. **92**, 511 (1954).

of a pion in order to obtain an estimate of the total energy taken by each particle.

The value of the visible outgoing energy from star *A* is considerably lower than the incident proton energy of 6.2 Bev. There is certainly sufficient energy available, after allowing for the energy of the visible prongs, for the production of a nucleon pair. At the same time, however, no conclusion from energetics alone can be reached as to whether track 9 is an antiproton of 710 Mev or some other higher energy particle capable of producing star *B*. The total visible energy in star *A*, including 1876 Mev required for antiproton-proton production, is only 4260 Mev. The total visible outgoing momentum of star *A* in the direction of the incident proton is only 3260 Mev/*c*, in the backward direction is 580 Mev/*c*, and the net momentum in the forward direction is therefore 2680 Mev/*c* as compared with an incident proton momentum of 7076 Mev/*c*. In the plane at right angles to the incident proton, the momentum is well balanced and of the order of 800 Mev/*c* in any particular direction in this plane.

Energy and momentum in star *A* cannot be balanced by assuming that as many neutrons as protons were emitted in the star and that the neutrons had energy and momentum distributions similar to the protons. Excluding the antiproton, only 600 Mev was carried off by the eight protons observed in star *A*. If eight 75-Mev neutrons were to have been emitted all in the forward direction, a very unlikely occurrence, there would still have been a large momentum deficiency of ~ 1350 Mev/*c* in the direction of the incident proton. The most reasonable assumption, consistent with the probable production dynamics of an antiproton, would seem to be that a single high-energy neutron, of the order 1 Bev or more, was emitted in the forward direction. A number of lower energy neutrons, with a more isotropic angular distribution, could also have been emitted to make up the balance of momentum and energy in the star.

Two interesting features concerning antiproton production in star *A* are that three pions are simultaneously produced and that the protons observed in the forward direction are of relatively low energies. For a proton of 6.2 Bev, colliding with a nucleon at rest in the laboratory system, the energy available in the center-of-mass system of the two nucleons after providing for nucleon-pair production is only 140 Mev. There is therefore insufficient energy for producing pions, for deflecting the nucleons taking part in the production process significantly from the direction of the incident proton, and for modifying the energies of the nucleons involved in the production process from the average value of approximately 1 Bev. Thus, in order to understand the production of an antiproton in star *A* in terms of a nucleon-nucleon collision, it seems necessary to assume that some of the protons involved in the production process interacted with other nucleons in emerging from the parent heavy nucleus.

For a nucleon Fermi energy of 25 Mev and a momen-

tum vector opposite to the direction of the incident 6.2-Bev proton, the energy available in the center-of-mass system of the two colliding nucleons is $4.6 Mc^2$. This would energetically allow the production of pions in association with nucleon-pair production. According to Fermi,⁴ the probability of single pion production accompanied by nucleon-pair production is $\sim 2 \times 10^{-4}$, in units of the total collision cross section, $\sim 6 \times 10^{-26}$ cm². The probability of zero-pion production accompanied by nucleon-pair production is $\sim 20 \times 10^{-4}$, in the same units. It seems unlikely, therefore, that the three pions observed in star *A*, could all have arisen in the initial nucleon-pair production process. This conclusion is also consistent with the fact that the nucleons involved in the antiproton production process must certainly

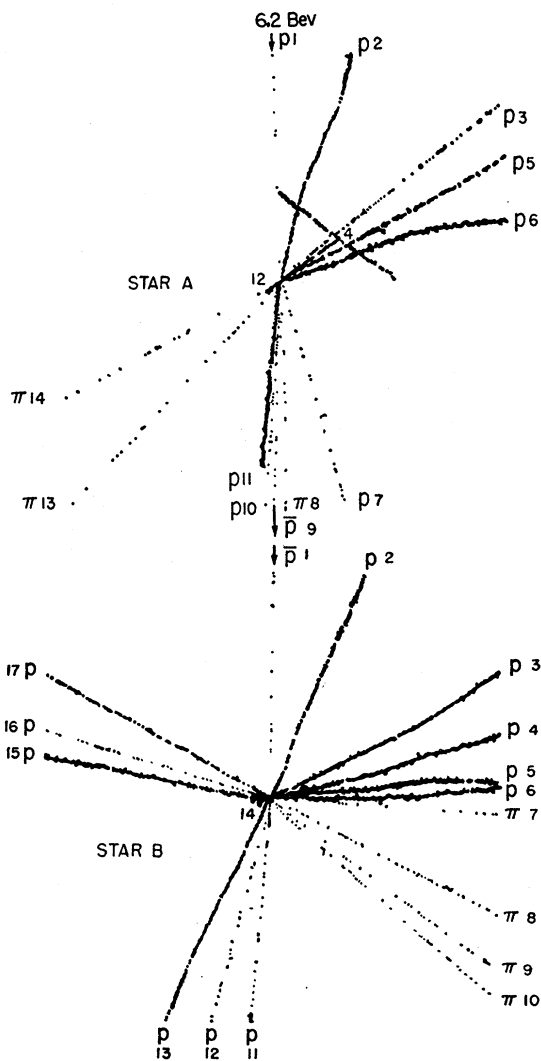


FIG. 1. Facsimile drawing of the observed antiproton event. The antiproton is created in star *A*, track 9, and is annihilated in star *B*, track 1, after passing 1.4 mm of emulsion. For explanation of the other tracks, see Tables I and IV.

⁴ E. Fermi, Prog. Theoret. Phys. Japan 5, 570 (1950).

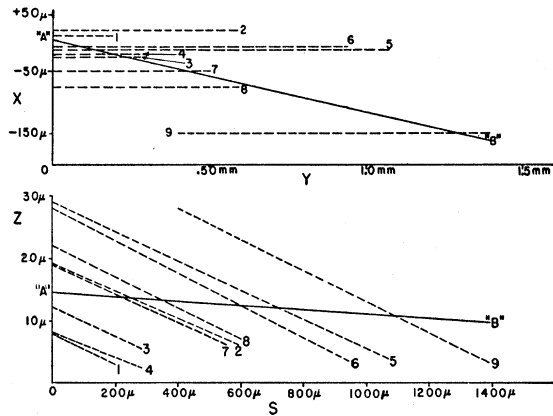


FIG. 2. The antiproton track (full line, $A-B$) with reference to beam protons (dotted lines) used in ionization density measurements. The X and Y coordinates are perpendicular to and along the direction of the 6.2-Bev protons. Coordinate Z refers to the height in the emulsion strip above the glass and S is along the projected length of the antiproton track.

have lost energies and have been deflected from their initial paths by interactions with other nucleons of the parent nucleus. The observed energies and angles of emergence of the protons which were most likely to have been involved in the nucleon-pair production process are: No. 9, antiproton, $E=710$ Mev, $\theta=7.2^\circ$; No. 7, proton, $E=290$ Mev, $\theta=14.8^\circ$; No. 10, proton, $E=123$ Mev, $\theta=27.8^\circ$. These values are not incompatible with a process in which at least one nucleon, and more probably two nucleons, involved in the production process subsequently interacted within the heavy nucleus.

ANTIPROTON TRACK

(a) Ionization Density Measurements

Except for the presence of standardizing 6.2-Bev proton tracks in the immediate vicinity of the anti-

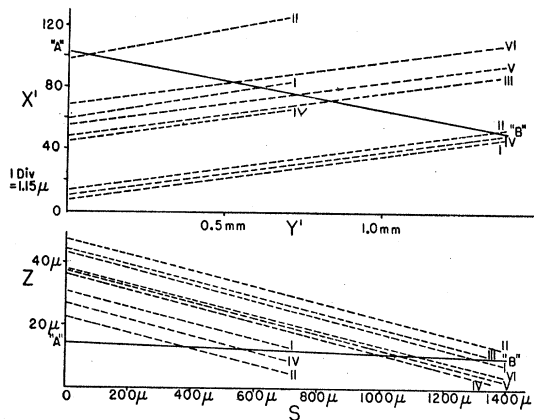


FIG. 3. The antiproton track (full line, $A-B$) with reference to beam protons (dotted lines) used in scattering measurements. The X' and Y' coordinates are perpendicular to and along the direction of motion of the scattering microscope stage. Coordinate Z refers to the height in the emulsion strip above the glass and S is along the projected length of the antiproton track.

TABLE II. Summary of scattering results (second differences).

(a) Antiproton vs 6.2-Bev beam protons				
	$\bar{D}_{200 \mu}$	$\bar{D}_{300 \mu}$	$\bar{D}_{400 \mu}$	$\bar{D}_{600 \mu}$
Mean (μ)	0.395	0.380	0.521	0.845
Error (μ)	0.135	0.150	0.230	0.640
(b) 6.2-Bev protons vs protons				
	$\bar{D}_{200 \mu}$	$\bar{D}_{300 \mu}$	$\bar{D}_{400 \mu}$	$\bar{D}_{600 \mu}$
Mean (μ)	0.316	0.261	0.302	0.252
Error (μ)	0.036	0.046	0.046	0.086

proton track, a reliable measurement of the ionization density of the antiproton track could not have been possible. The positions of the calibrating beam protons relative to the antiproton track joining stars A and B are shown in Fig. 2. A total of 1196 blobs were counted in 5400 μ of proton tracks distributed equally above and below the antiproton track. In the 1400 μ of the antiproton track there were 352 blobs. The blob density of the antiproton track was therefore 25.4 ± 1.1 blobs per 100 μ , and the 6.2 Bev proton blob density was 22.1 ± 0.5 blobs per 100 μ . If the 6.2-Bev protons are assumed to have an ionization density 5% below plateau ionization,³ the antiproton ionization density is 9% above plateau and its energy is 710 Mev.⁵

(b) Scattering Measurements

The antiproton track is 1.4 mm long and dips 2 μ , in the developed emulsion, along its whole length. The path of the antiproton between stars A and B is shown in Fig. 3. Also shown in the figure are high-energy (6.2-Bev) proton tracks at an angle of approximately 7° to the antiproton track, and with reference to which the scattering of the antiproton track was measured using a track-to-track type of measurement. Each scattering measurement with reference to a particular proton was carried out a number of times. The average values of the mean second differences of the antiproton track compared to six beam proton tracks are given for different lengths of cells in Table II(a). The standard deviation errors were obtained from the number of

TABLE III. Mean scattering angle $\bar{\alpha}_{100 \mu}$ for antiproton track.

(i) From noise subtraction				
Cell length	200 μ	300 μ	400 μ	600 μ
$\bar{\alpha}_{100 \mu}$	0.047°	0.031°	0.031°	0.032°
Error	0.028°	0.017°	0.017°	0.025°
(ii) From noise elimination				
Cell lengths	200 μ -400 μ		300 μ -600 μ	
$\bar{\alpha}_{100 \mu}$	0.026°		0.033°	
Error	0.021°		0.028°	

⁵ Owing to a slight reassessment of the calibration curve³ above plateau, this energy value is slightly lower than that previously reported.¹ The error, on the basis of a 5% standard deviation in blob density, is of the order of ± 100 Mev.

TABLE IV. Details of tracks of star *B*.

Track	Identity	Range	Plates	Dip angle ^a	Space angle to track No. 1.	Grain or blob count ^b	Ionization $p\beta$ (Mev/c)	Scattering $p\beta$ (Mev/c)	Momentum (Mev/c)	Energy (Mev)	Total energy (Mev)
1	\bar{p}	(1.4 mm)	20	0.02°	...	(1.09±0.05) b_p	(1115±150)	(750 ₋₂₄₀ ⁺⁶⁷⁰)	1355	710	
2	p	194 μ	20,21	6°	24°	101	5.4	13.4
3	p	173 μ	20	9°	63°	98	5.1	13.1
4	p	2.3 mm	20-15	64°	84°	209	22.9	30.9
5	p	763 μ	20,19	65°	86°	152	12.2	20.2
6	p	964 μ	20-18	60°	90°	162	13.9	21.9
7	π	>20 mm	20-1	21°	93°	(1.01±0.03) b_p	(185 ₋₁₆ ⁺⁴⁰)	(120 ₋₂₅ ⁺⁴⁰)	226	126	266
8	π	>12.5 mm	20-1	39°	109°	(1.62±0.08) g_p	(90±10)	(125 ₋₃₆ ⁺⁸⁰)	130	51	191
9	π	>15.9 mm	20-1	28°	120°	(1.38±0.06) g_p	(125±10)	(270 ₋₆₀ ⁺¹⁰⁰)	162	74	214
10	π	>1.85 mm	20-24	59°	103°	(1.50±0.11) g_p	(105±15)	(40 ₋₁₅ ⁺⁴⁰)	145	62	202
11	p	>30 mm	20-15	6°	168°	(2.54±0.09) g_p	(235±20)	(230 ₋₃₀ ⁺⁴⁰)	509	129	137
12	p	>30 mm	20-4	12°	162°	(2.32±0.08) g_p	(270±20)	(235 ₋₃₆ ⁺⁵⁰)	546	147	155
13	p	63 μ	20	flat	152°	71	2.7	10.7
14	$\alpha?$	4 μ	20	flat	116°	109	1.6	3.6
15	p	1.18 mm	20-23	57°	84°	172	15.6	23.6
16	p	>14.8 mm	20-24	6°	74°	(2.72±0.09) g_p	(210±15)	(130±30)	474	113	121
17	p	4.66 mm	20-14	24°	65°	255	34	42

^a Dip angles are in the undeveloped emulsion.

^b b_p and g_p refer to the plateau values of blob and grain densities, respectively.

independent cells of the antiproton track only. The scattering of the same proton tracks, as used in the foregoing, were measured with reference to one another in a number of combinations. The scattering was measured only for those lengths which covered the same region of the emulsion as the antiproton track. The averages of the second differences for different cell lengths are given in Table II(b). The standard deviation errors in these cases are based on the numbers of independent cells for the six proton tracks.

It is significant that, whereas the mean second differences for the proton track-to-track scattering remain sensibly constant with length of cell, the second differences for the antiproton track scattering increase with increasing cell length.⁶ The mean scattering angles, $\bar{\alpha}_{100\mu}$, for the antiproton track were obtained from the data of Table II in two ways. The values of $\bar{\alpha}_{100\mu}$ obtained from Table II(a) by subtraction of the appropriate noise of part (b) are given in Table III (i). The values of $\bar{\alpha}_{100\mu}$ obtained from Table II(a) by noise elimination between two different cell lengths are given in Table III (ii). These values of $\bar{\alpha}_{100\mu}$ are consistent

⁶ In other direct scattering experiments on high-energy beam proton tracks, a value of 0.18 μ has been obtained for scattering noise. A value of $\sim 0.3\mu$ for track-to-track scattering noise is therefore reasonable. Our noise is mainly attributable to grain noise. We use an internal scale instead of a goniometer line for locating the y -coordinate of a track. In the presence of this comparatively large grain noise, there is no evidence from Table II(b) of increase of noise due to stage noise or to reading noise for cells up to lengths of $\sim 600\mu$.

with one another, and, although the accuracy of the scattering on account of the short length of track is not high, point to a reliable evaluation of the multiple scattering of the antiproton track. The weighted mean scattering angle is 0.032°, with an estimated standard deviation of the order of 0.015°. For a scattering constant of 24.1, we obtain for $p\beta$ of the antiproton track a value of (750₋₂₄₀⁺⁶⁷⁰) Mev/c. The $p\beta$ value from ionization density measurements, assuming a proton mass and an energy of 710 Mev, is (1115±150) Mev/c.

ANNIHILATION STAR

The information concerning the annihilation star is summarized in Table IV. These results are practically the same as given previously,¹ except that for some tracks more accurate grain density measurements have been made. On the basis of the variation of ionization density vs range, tracks 11, 12, and 16 have been conclusively identified as protons, and for tracks 8 and 9 there is strong support for the identification of these tracks as pions by means of ionization density vs scattering. The revised value for the total visible energy release in star *B*, including proton binding energies and pion rest energies, is 1460 Mev.

ACKNOWLEDGMENTS

We are indeed deeply grateful to all those members of the Radiation Laboratory, University of California, who have made these experiments possible.